

## TRANSIENT AND STATIONARY NUTATIONS IN CHEMICALLY INDUCED DYNAMIC NUCLEAR POLARIZATION\*

Hanns FISCHER and Gary P. LAROFF

*Physikalisch-Chemisches Institut der Universität Zürich, CH-8001 Zurich, Switzerland*

Received 17 September 1973

Transient nutations are observed in nuclear magnetic resonance during continuous generation of magnetization at and near resonance in reactions leading to chemically induced dynamic nuclear polarization. Modulation of the reaction with the nutation frequency leads to stationary nutations. The phase-sensitive detection of the nutation signals is used to discriminate effects of chemically induced polarization from steady state resonance signals. For single line spectra the effects are quantitatively explained by Bloch-type equations containing magnetization production terms. Experimental results obtained during photochemical reactions of di-tert-butyl ketone demonstrate general applications of the method.

### 1. Introduction

A two-energy level system suddenly subjected to a strong coherent radiation field of the transition frequency approaches steady state through oscillations damped by relaxation. These transient oscillations have first been observed in nuclear magnetic resonance [4], and were detected more recently in laser [5, 6] and microwave spectroscopy [7]. In nuclear magnetic resonance they represent the initial part of the motion of the magnetization vector, and appear as transient nutations superimposed on the rapid precession about the axis of the static magnetic field. As Torrey [4] has shown for simple systems, the effects are quantitatively explained in the frame of the Bloch theory, and he has given the explicit transient solutions of the Bloch equations for a number of special cases. Applications of the transient nutations include determinations of relaxation times [4, 8, 9] and the strength,  $H_1$ , of the radiofrequency field [10]; in double resonance, assignments of the transitions in energy level diagrams and the signs of spin coupling constants [11, 12] are also obtainable.

The transient situation may be set up by any approach to the resonance condition which is rapid compared to the nutation period. In conventional

nuclear magnetic resonance any one of the three external parameters  $H_0$ ,  $H_1$  or the radiation frequency  $\omega$  may be varied with time in the pulse form [4]. As a fourth possibility we may consider a rapid change of the magnitude of magnetization at resonance. In this paper we verify this situation in experiments dealing with chemically induced dynamic nuclear polarization (CIDNP) where products of chemical reactions carrying large nuclear polarizations are rapidly formed at resonance. We will also show that a suitable modulation of the reaction leads to stationary nutations, the phase-sensitive detection of which can be used to discriminate CIDNP-signals from signals of unpolarized species.

In section 2 of this paper the formulae necessary to explain the effects are derived from Bloch's theory modified by additional terms to allow for the production of magnetization by the reactions. The mathematical treatment closely follows Torrey's original work [4]. To account for transient electron spin polarization effects Fessenden et al. [13] and Atkins et al. [14] have recently performed calculations related to our work. Section 3 describes the experimental procedures. In section 4 experimental results obtained during photolysis of di-tert-butyl ketone in  $\text{CCl}_4$  are presented and compared with the theoretical expectation. We have chosen this particular chemical system because of its strong CIDNP-effects which have been studied before to some detail [15–17] and

\* 16th communication on chemically induced dynamic nuclear polarization. Parts 13–15: refs. [1–3].

because a variety of applications of the stationary nutations can be demonstrated with this system.

## 2. Theory

The following treatment is restricted to a two-level system of spin  $I = \frac{1}{2}$  nuclei subject to interactions with the static field  $H_0$  ( $Z$ -direction) and the oscillating field,  $2H_1 \cos \omega t$ , to relaxation and to reaction. In the absence of reaction the Bloch equations

$$dM_X/dt = (\gamma H_0 - \omega)M_Y - M_X/T_2, \quad (1.1)$$

$$dM_Y/dt = -(\gamma H_0 - \omega)M_X + \gamma H_1 M_Z - M_Y/T_2, \quad (1.2)$$

$$dM_Z/dt = -\gamma H_1 M_Y - (M_Z - M_Z^0)/T_1, \quad (1.3)$$

describe the motions of the components of the magnetization vector in the right-handed coordinate system  $X, Y, Z$  rotating about  $Z$  in the same sense as the free Larmor precession. We will be particularly interested in solutions for the component  $M_Y$  which is perpendicular to the effective component of the oscillating field ( $X$ ), since this will be the observable quantity. Torrey [4] has given an implicit and several explicit solutions of (1). For instance at resonance  $\gamma H_0 = \omega$  and for the initial condition  $M = \{0, 0, M_Z^0\}$  at  $t \leq 0$ :

$$M_Y = \{\alpha M_Z^0 / (1 + \alpha\beta)\}$$

$$\times \left\{ 1 - e^{-\sigma t} \left[ \cos \rho t - \frac{1}{\rho} \left( \frac{1 + \alpha\beta}{\alpha} - \sigma \right) \sin \rho t \right] \right\}, \quad (2)$$

where

$$\omega_1 = \gamma H_1, \quad \alpha = 1/\omega_1 T_1, \quad \beta = 1/\omega_1 T_2, \quad \tau = \omega_1 t.$$

The angular frequency of the nutations is given by

$$\rho \omega_1 = \{\omega_1^2 - \frac{1}{4}(1/T_1 - 1/T_2)^2\}^{1/2} \quad (3)$$

and becomes equal to  $\omega_1$  for sufficiently large  $H_1$  or sufficiently long relaxation times, whereas the damping constant is

$$\sigma \omega_1 = \frac{1}{2}(1/T_1 + 1/T_2). \quad (4)$$

Off resonance a faster damping of the nutations occurs. For sufficiently long relaxation times the frequency is then approximately given by

$$\rho \omega_1 = \{\omega_1^2 + (\omega - \gamma H_0)^2\}^{1/2}. \quad (5)$$

To account for the presence of chemical reactions we now introduce reaction terms in eqs. (1). Since, according to the theory of CIDNP [18–20] the individual product molecules of the spin ensemble are formed in individual uncorrelated reaction events there will be no creation terms for the off-diagonal elements of the density operator in the representation of eigenstates of  $I_Z$ . Therefore, we have to consider only the formation of magnetization along the  $Z$ -direction, i.e., to introduce a reaction term in eq. (1.3) only. In the following we will use eqs. (1.1) and (1.2) as stated and replace (1.3) by

$$dM_Z/dt = -\gamma H_1 M_Y - (M_Z - M_Z^0)/T_1 + r, \quad (1.4)$$

where  $r$  is the creation rate of  $M_Z$ ;  $r$  can be expressed in CIDNP terms but will be used here as an empirical parameter.

In the following we will consider the cases of (A) continuous reaction, i.e.,  $r = \text{constant}$  for a time interval long compared to the period of the transient nutation and (B) modulated reaction with  $r = r(t)$  modulated with frequencies of about the nutation frequency. Further we consider the case of a reaction product with an enhancement factor so large that  $M_Z^0$  can be neglected in (1.4).

### (A) Continuous reaction. Direct observation of the transient nutations

Following Torrey's procedure [4] eq. (1.1), (1.2) and (1.4) are solved via Laplace transformation for the conditions  $t \leq 0: M = 0, r = 0$  and  $t > 0: r = \bar{r} = \text{const.}$  For exact resonance,  $\omega = \gamma H_0$ , we obtain

$$M_X = 0, \quad (6.1)$$

$$M_Y = \{\bar{r} / \omega_1 (1 + \alpha\beta)\} \{1 - e^{-\sigma t} [\cos \rho t + (\sigma/\rho) \sin \rho t]\}, \quad (6.2)$$

$$M_Z = \{\bar{r} \beta / \omega_1 (1 + \alpha\beta)\} \times \left\{ 1 - e^{-\sigma t} \left[ \cos \rho t - \frac{1}{\rho} \left( \frac{1 + \alpha\beta}{\beta} - \sigma \right) \sin \rho t \right] \right\}. \quad (6.3)$$

The abbreviations  $\alpha, \beta, \sigma, \rho$  and  $\tau$  are the same as before. Obviously, the transient nutations of the magnetization do appear before the steady state

$$\bar{M}_X = 0, \quad (7.1)$$

$$\bar{M}_Y = \frac{\bar{r}}{\omega_1(1+\alpha\beta)} = \frac{\bar{r}\omega_1 T_1 T_2}{1+\omega_1^2 T_1 T_2}, \quad (7.2)$$

$$\bar{M}_Z = \frac{\bar{r}\beta}{\omega_1(1+\alpha\beta)} = \frac{\bar{r}T_1}{1+\omega_1^2 T_1 T_2} \quad (7.3)$$

is reached.

If the reaction is interrupted at a time  $t'$  the magnetization returns to zero, again after transient nutations. To show this we solve (1) with the initial condition  $t \leq t'$ :  $r = \bar{r}$ ,  $M = \{\bar{M}_X, \bar{M}_Y, \bar{M}_Z\}$  and  $t > t'$ :  $r = 0$  and find for exact resonance

$$M_Y = \{\bar{r}/\omega_1(1+\alpha\beta)\} e^{-\sigma(\tau-\tau')} \times \{\cos \rho(\tau-\tau') - (\sigma/\rho) \sin \rho(\tau-\tau')\}. \quad (8)$$

As is clearly seen from (6) to (8) the amplitudes of the oscillations may be as large as the steady state CIDNP signal. Therefore they should be easily observable.

#### (B) Modulated reaction. Phase sensitive detection of the transient nutations

We assume that for  $t \leq 0$ :  $M = 0$  and  $r = 0$ , whereas for  $t > 0$ :  $r = r(t) = \sum_{n=0}^{\infty} r_n \cos n\omega_m t$  where  $n = 1$  denotes the first harmonic of the modulation. The amplitudes  $r_n$  of the individual Fourier components shall be time independent. Using Laplace transformation as before and the substitution  $m = \omega_m/\omega_1$  we obtain from (1) for exact resonance

$$M_Y = \sum_{n=0}^{\infty} (r_n/\omega_1 B_n) \{(1+\alpha\beta-n^2 m^2) \times (\cos nm\tau - e^{-\sigma\tau} \cos \rho\tau) + \sigma[2nm \sin nm\tau - (1/\rho)(1+\alpha\beta+n^2 m^2)e^{-\sigma\tau} \sin \rho\tau]\}, \quad (9)$$

where

$$B_n = (1+\alpha\beta-n^2 m^2)^2 + 4\sigma^2 n^2 m^2.$$

Eq. (9) shows the appearance of decaying nutations of

angular frequency  $\rho\omega_1$  and of stationary nutations of the modulation frequencies  $n\omega_m$ . For an arbitrary frequency  $\omega \neq \gamma H_0$  and modulation  $r(t)$ , integration of (1) via Laplace transformation becomes rather tedious. Since we will be interested in the stationary nutations of the modulation frequencies and not in terms decaying with time we only have to look for solutions of the type

$$M_X = \sum_n (M_{Xn}^C \cos n\omega_m t + M_{Xn}^S \sin n\omega_m t), \quad (10.1)$$

$$M_Y = \sum_n (M_{Yn}^C \cos n\omega_m t + M_{Yn}^S \sin n\omega_m t), \quad (10.2)$$

$$M_Z = \sum_n (M_{Zn}^C \cos n\omega_m t + M_{Zn}^S \sin n\omega_m t). \quad (10.3)$$

Insertion of (10) into eqs. (1.1), (1.2) and (1.4) with  $r = \sum_n r_n \cos n\omega_m t$  and use of the orthogonality of the trigonometric functions leads to a set of six coupled linear equations for the amplitudes of eqs. (10), the solution of which is straightforward and leads to

$$M_{Yn}^C = (r_n/\omega_1 D_n) \{(\beta^2+n^2 m^2)(1+\alpha\beta-n^2 m^2) + \Delta^2(\alpha\beta+n^2 m^2)\}, \quad (11.1)$$

$$M_{Yn}^S = (r_n n m/\omega_1 D_n) \{(\beta^2+n^2 m^2)2\sigma + \Delta^2(\beta-\alpha)\}, \quad (11.2)$$

where

$$D_n = (\beta^2+n^2 m^2)(1+\alpha\beta-n^2 m^2)^2 + 4\sigma^2 n^2 m^2 + 2\Delta^2 \{(\beta^2-n^2 m^2 + \frac{1}{2}\Delta^2)(\alpha^2+n^2 m^2) + \alpha\beta+n^2 m^2\} \quad (11.3)$$

and

$$\Delta = (\omega - \gamma H_0)/\omega_1.$$

Similar equations hold for the  $M_X$ - and  $M_Z$ -terms; they are not given here because they are not needed in the following.

Though the expressions (11) have a rather complicated appearance the dependence of  $M_{Yn}^C$  and  $M_{Yn}^S$  on the modulation frequency  $\omega_m = m\omega_1$  and on the offset from resonance  $\omega - \gamma H_0 = \Delta\omega_1$  is fairly simple and can be seen most easily if long relaxation times

are assumed ( $\alpha, \beta \ll 1$ ). For the first harmonic  $n = 1$  and modulation frequencies  $\omega_m$  smaller than  $\omega_1$  ( $m \ll 1$ ) the amplitude  $M_{Y1}^S$  of the out-of-phase term is a resonance type absorption function of the offset  $\Delta\omega_1$ .  $H$  reaches its maximum amplitude at  $\omega = \gamma H_0$  for  $\omega_m = \omega_1$  ( $m = 1$ ). With  $m$  increasing in the range  $m > 1$  the absorption curve splits into two lines with maxima at

$$\Delta\omega_1 = \omega - \omega_0 = \pm \{\omega_m^2 - \omega_1^2\}^{\frac{1}{2}}. \quad (12)$$

This behavior is easily understood in terms of eqs. (3) and (5): maximum absorption occurs if the modulation frequency  $\omega_m$  is equal to the frequency of the transient nutations  $\rho\omega_1$ .

The in-phase term shows a more complicated variation with  $m$ . For  $m \ll 1$  and  $n = 1$  again a resonance type absorption function of  $\Delta\omega_1$  is found. As  $m$  increases  $M_{Y1}^C$  develops a minimum at resonance  $\Delta\omega_1 = 0$ . For  $m > 1$  zero crossing points are found at the maxima positions of  $M_{Y1}^S$  (12).

In section 4 we will display  $M_{Y1}^S$  and  $M_{Y1}^C$  as functions of  $\Delta\omega_1$  for various values of  $\omega_m$  and compare the results with experimental findings (figs. 4 and 5), obtained by phase-sensitive detection on the modulation frequency.

It is interesting to compare the optimum value of  $M_{Y1}^S$  at  $\Delta\omega_1 = 0$  and  $\omega_m = \omega_1$  with the optimum value of  $\bar{M}_Y$  for continuous reaction and long relaxation times.

Eq. (7.2) shows that for low  $H_1$ -field, i.e., no saturation,

$$\bar{M}_Y = \bar{r} \omega_1 T_1 T_2. \quad (13)$$

The proportionality to the longitudinal relaxation time has been derived previously by kinetic arguments [21, 22]. The optimum signal intensity is obtained for partial saturation  $\omega_1^2 T_1 T_2 = 1$  and is given by

$$\hat{M}_Y = \frac{1}{2} \bar{r} (T_1 T_2)^{\frac{1}{2}}. \quad (14)$$

The amplitude  $M_{Y1}^S$  at  $m = 1$  and  $\Delta = 0$  follows from (11.2) and (11.3) as

$$M_{Y1}^S = r_1 \frac{\omega_1^2 T_1 T_2 (T_1 + T_2)}{1 + \omega_1^2 (T_1 + T_2)^2} \quad (15)$$

and reaches an optimum value for saturation conditions  $\omega_1^2 (T_1 + T_2)^2 \gg 1$

$$\hat{M}_{Y1}^S = r_1 T_1 T_2 / (T_1 + T_2). \quad (16)$$

If we assume a harmonic modulation of the reaction of the type

$$r(t) = \frac{1}{2} \bar{r} (1 + \cos \omega_m t),$$

we find

$$\hat{M}_{Y1}^S = \{(T_1 T_2)^{\frac{1}{2}} / (T_1 + T_2)\} \hat{M}_Y; \quad (17)$$

on the other hand, for a square wave modulation

$$r(t) = \frac{1}{2} \bar{r} + (\bar{r}/\pi) \sum_{n=1}^{\infty} (1/n)$$

$$\times (\sin \frac{1}{2} n \pi - \sin \frac{3}{2} n \pi) \cos n \omega_m t,$$

one obtains

$$\hat{M}_{Y1}^S = (4/\pi) \{(T_1 T_2)^{\frac{1}{2}} / (T_1 + T_2)\} \hat{M}_Y. \quad (18)$$

Since  $(T_1 T_2)^{\frac{1}{2}} (T_1 + T_2)^{-1} \leq \frac{1}{2}$ , (17) and (18) show that  $\hat{M}_{Y1}^S$  will be smaller than  $\hat{M}_Y$  and the phase-sensitive detection will be less sensitive than the normal mode. However, in general, the loss of sensitivity will not be very large.

### 3. Experimental

A 100 MHz proton NMR spectrometer (Varian HA 100 D) was used in frequency sweep mode and set for the detection of  $M_Y$ . It was equipped with a room temperature probe (Varian V 4332) modified to allow UV irradiation of sample solutions in the region of the receiver coil [17]. The light of a water-cooled mercury high pressure lamp (Philips SP 1000 W) filtered by an Ni/CoSO<sub>4</sub>/H<sub>2</sub>O solution [23] to eliminate the infrared, and part of the visible light was focused by lenses onto the front end of a suprasil quartz rod which served as a light pipe to the sample. The spectral distribution of the ultraviolet radiation was published earlier [24].

The samples were 0.12 M solutions of di-tert-butyl ketone in 80% carbon tetrachloride and 20% octa-tetramethyl siloxane the latter of which served as an internal lock signal. All chemicals were purchased from Fluka in the purest available form and used without further purification.

The longitudinal relaxation time  $T_1$  of tert-butyl

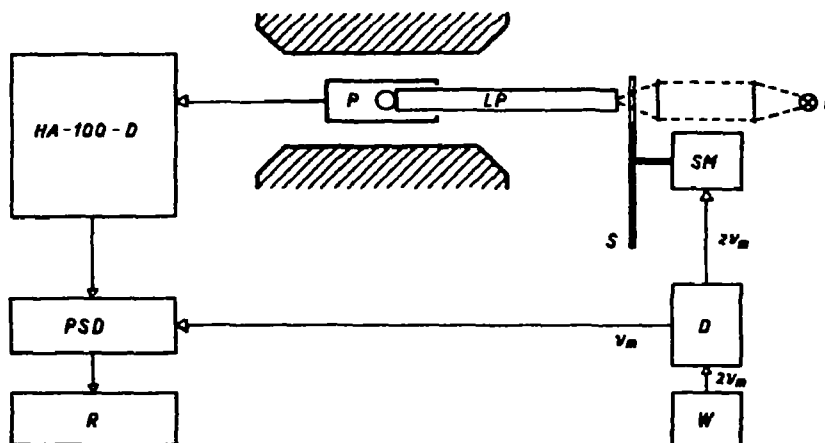


Fig. 1. Arrangement for the observation of stationary nutations in a modulated photo-reaction.

chloride was measured by a rapid passage technique [25] using photolyzed samples of the ketone in  $\text{CCl}_4$  and was found to be  $T_1 = (9.4 \pm 0.3)$  sec. Under typical experimental conditions the linewidths of single lines were in the range of 0.30 to 0.45 Hz. The  $H_1$ -field was measured by Torrey's method [10]. To observe the transient nutations of photochemically induced magnetization (case A of section 2) the spectrometer was set prior to irradiation to the resonance condition of the line to be observed. The  $H_1$ -field was set to  $H_1 = 0.203$  mG, and the dc output of the spectrometer was connected to the  $y$ -axis of a  $y$ - $t$  recorder (Servogor R 541, Goerz). The nutations appeared at the start of the irradiation.

For phase-sensitive detection of the stationary nutations in modulated reactions (case B) the arrangement shown in fig. 1 was used. In front of the quartz rod (LP) the light was chopped with a sector (S) driven by a stepper motor (Philips Polymotor ID 08) to ensure a square-wave type modulation. Two steps of the motor comprise one cycle of the modulation. The motor frequency  $2\nu_m$  was taken from a voltage controlled frequency generator (Wavetec model 111) through a driving unit D containing electronic switches of the motor and a frequency divider to generate  $\nu_m$ . The spectrometer signal carrying the nutations was fed into a low-frequency lock-in amplifier (PSD) (Ithaco Model 391 A) which was driven by  $\nu_m$ , and the rectified signal was displayed on the external Servogor recorder (R). Scanning through resonance was accomplished as

usual via the recorder of the spectrometer. The time-constant of detection was 4 sec, and therefore the low scanning speed of  $2 \times 10^{-2}$  Hz/sec was used. In all experiments the  $H_1$ -field was set to 0.203 mG.

## 4. Results and discussion

### 4.1. Photochemical reactions of di-*tert*-butyl ketone in carbon tetrachloride

The photolysis leads to *tert*-butyl chloride as one of the major products, and the proton CIDNP-effects have been described in part by Cocivera et al. [15, 16] and more fully by Blank [17]. In the usual nomenclature (A: enhanced absorption, E: emission and A/E: emission/absorption type multiplet effects [26]) they are: A for the ketone 1, E for *tert*-butyl chloride 2, A + A/E for isobutene 3 ( $\text{CH}_3$ - and  $\text{CH}_2$ -groups), A for the CHO-proton and E for the  $\text{CH}_3$ -protons of pivalaldehyde 4, A for chloroform 5 and A for trichloro neopentane 6. The upper part of fig. 2 shows these effects. With the aid of the simple rules of CIDNP-theory [26] and the known radical parameters they are easily explained by the reactions of scheme I ( $\text{R} = \text{C}(\text{CH}_3)_3$ ).

The importance of the pair  $\text{RCO } \dot{\text{R}}^{\text{T}}$ , derived from a triplet state of 1 and leading to polarized 2, 3 and 4, has been noted before [15, 16] but these authors did not report on the weak enhanced absorption of

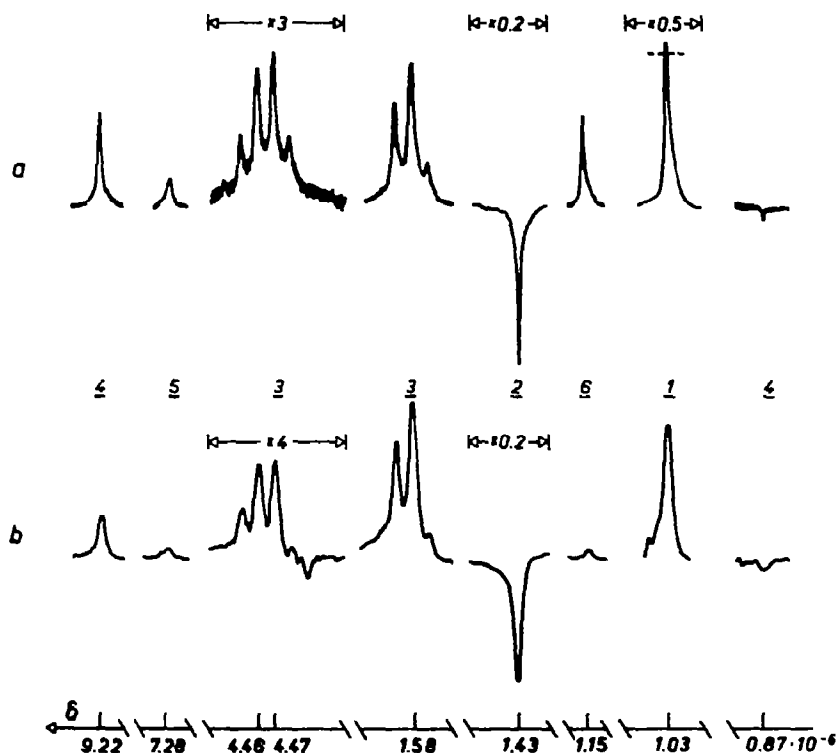
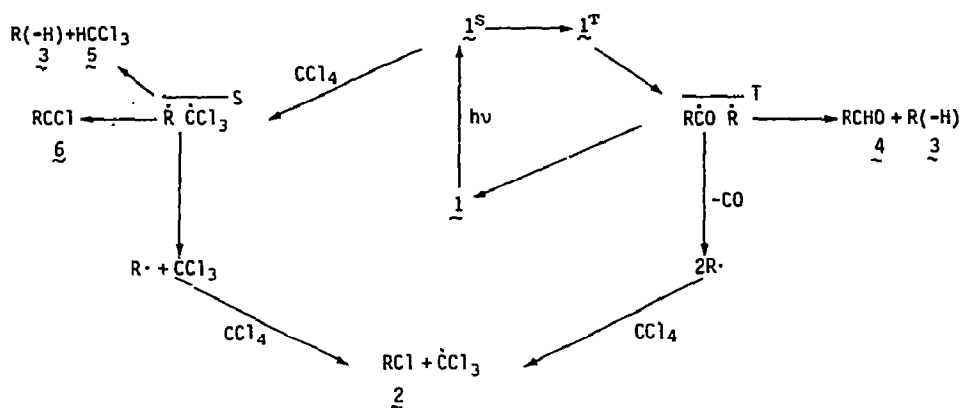


Fig. 2. CIDNP-effects during the photolysis of di-tert-butyl ketone in carbon tetrachloride (6 referenced to TMS, assignments: see text section 4.1, spectrometer gain as indicated, scan rate  $2 \times 10^{-2}$  Hz/sec for (a) and (b), the individual groups of transitions were observed each with fresh samples approximately two minutes after onset of the photoreactions). (a) Steady state spectra during continuous photolysis (— amplitude before photolysis); (b) nutation spectrum during modulated photolysis ( $\nu_m = 0.99\nu_1$ ).

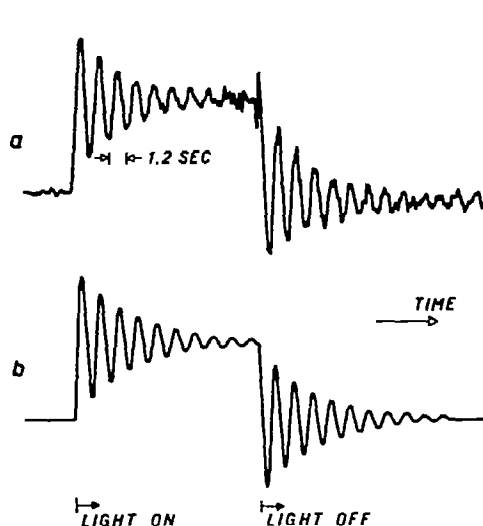


Fig. 3. Transient nutations (a) observed for the emission of tert-butylchloride during and after photolysis of di-tert-butyl ketone in carbon tetrachloride. (b) Calculated from eqs. (6.2) and (8).

1 which corresponds to the regeneration of the ketone from that pair. The singlet reaction on the left side of the scheme presumably has a singlet exciplex precursor as with other ketones [17, 27]. It seems to be the only reasonable mechanism leading to the enhanced absorptions of 5 and 6 which seem to have hitherto escaped attention [15, 16]. It is further supported by results of experiments with variable  $\text{CCl}_4$ -concentrations [17].

#### 4.2. Transient nutations during continuous reaction

Fig. 3a shows the transient nutations observed for the emission line of tert-butyl chloride 2 at exact resonance after the onset and after the end of photolysis of 1 in  $\text{CCl}_4$ . The signal returns to the baseline after the end of the cycle. This demonstrates negligible product formation and justified the choice of  $M_2^0 = 0$  for that case. Fig. 3b displays a simulation of the transient effect which is based on the appropriate formulae (6.2) and (8), the frequency  $\nu_1 = \omega_1/2\pi = \gamma H_1/2\pi = 0.865$  Hz, the longitudinal relaxation time  $T_1 = 9.4$  sec (section 3), a scaling factor  $\bar{r}$ , and  $T_2 = 2.3$  sec as the only important fitting parameter. Obviously,

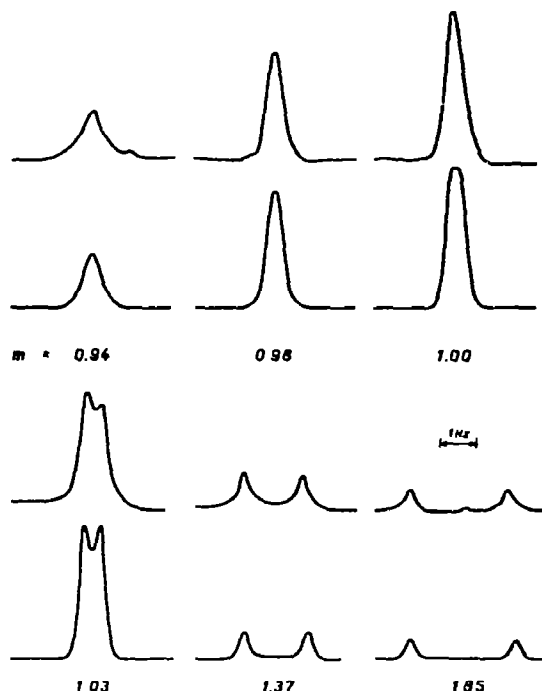


Fig. 4. Experimental and theoretical amplitudes of the out-of-phase term  $M_{Y1}^S$  of stationary nutations for tert-butyl chloride as functions of the rf-frequency  $\nu$  for various modulation frequencies of the photolysis  $\nu_m = m\nu_1$ .

in the present case,  $\alpha = 0.0195$  and  $\beta = 0.0795$  are both small compared to unity so that the frequency of the nutation is determined by  $\gamma H_1$  and the condition of long relaxation times is applicable. As expected, the amplitude of nutation is of the order of magnitude of the steady state CIDNP-signal.

#### 4.3. Stationary nutations

To investigate the validity of the theoretical formulae (11), the amplitudes of stationary nutations  $M_{Y1}^S$  and  $M_{Y1}^C$  were recorded as functions of the frequency  $\omega - \omega_0 = \Delta\omega_1$  for the emission signal of tert-butyl chloride and various modulation frequencies  $\omega_m = m\omega_1$ .  $H_1 = 0.203$  mG and the same spectrometer settings were used in all experiments. Figs. 4 ( $M_{Y1}^S$ ) and 5 ( $M_{Y1}^C$ ) show the experimental results together with curves calculated from eqs. (11) with the previously determined  $\nu_1 = 0.865$  Hz,

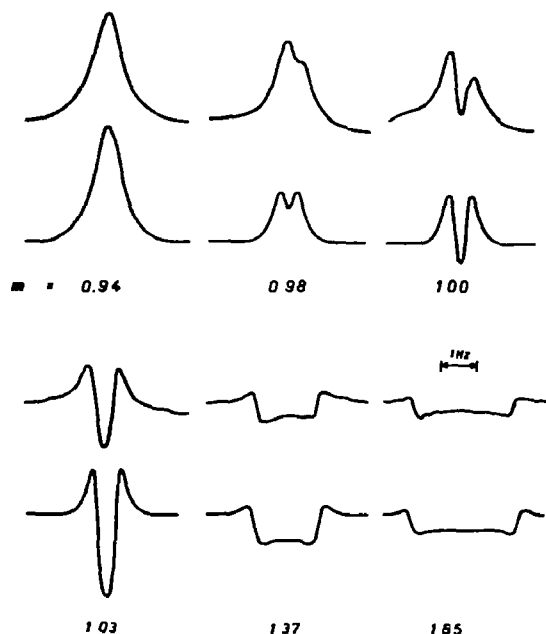


Fig. 5. Experimental and theoretical amplitudes of the in-phase term  $M_{Y_1}^S$  of stationary nutations for tert-butyl chloride as functions of the rf-frequency  $\nu$  for various modulation frequencies of the photolysis  $\nu_m = m\nu_1$ .

$T_2 = 2.3$  sec and  $T_1 = 9.4$  sec. One scaling factor for the amplitudes was adjusted to give a best fit for the amplitude of  $M_{Y_1}^S$  at resonance and  $m = 1$ . We feel that the agreement of calculated with experimental curves is very gratifying. Small asymmetries of the experimental curves are due to small inhomogeneities of the static  $H_0$ -field.

Fig. 6 shows the amplitude of the out-of-phase term  $M_{Y_1}^A$  at resonance as a function of the modulation frequency  $\nu_m = m\nu_1$  together with the calculated function. In fig. 7 the displacement of the maxima of  $M_{Y_1}^S$  from resonance,  $\nu_0 = \gamma H_0 / 2\pi$ , for  $m > 1$  is plotted versus the modulation frequency  $\nu_m$ . A plot of  $(\nu - \nu_0)^2$  versus  $\nu_m^2$  was chosen to demonstrate that the experimental data fit the straight line of slope unity, which is expected from eq. (12). The small deviations found for large  $\nu_m$  are probably due to a very slightly incorrect phase-setting of the lock-in amplifier.

The following experiments were carried out to demonstrate the possible applications of the stationary nutation method in CIDNP-studies. Part (a) of fig. 8

shows the emission line of tert-butyl chloride recorded as a function of time during continuous photolysis by repeatedly scanning through resonance under conventional NMR-conditions. After starting the irradiation the emission develops rapidly to its maximum value. Thereafter it shows a slow decay, and after about 17 minutes an absorption line is observed which continuously gains intensity. This is due to the build-up of tert-butyl chloride as the major reaction product and to the relaxation of the polarization towards the equilibrium value. The three lines at the end of the recording period show the intensity of the signal after irradiation. The sudden increase after the interruption of photolysis shows that the absorption lines observed after 17 minutes of photolysis still carry a substantial emissive polarization. Part (b) of fig. 8 shows the development of the stationary nutation amplitude  $M_{Y_1}^S$  during modulated photolysis for the same time interval. Obviously the emissive part of the signal can now be observed over the full time interval. After photolysis and relaxation to thermal equilibrium, no trace of a signal is detected. Thus the transient nutation method can be applied to discriminate the CIDNP-part of an NMR-signal from the part corresponding to an equilibrium polarization.

This feature is particularly useful to detect weak CIDNP-signals of reagents which are regenerated in the course of the reactions. In our system this is the case with di-tert-butyl ketone (see scheme 1) which exhibits a weak enhanced absorption detectable only immediately after the start of the photolysis. This weak enhanced absorption is demonstrated in fig. 1 and in part (a) of fig. 9 which shows the time development of the NMR-signal of the ketone. Only the first trace after the start of the reaction exhibits an obvious enhancement whereas all later traces show signals about equal to or smaller than the initial ketone line, because the ketone is rapidly decomposed. The lower part, (b), of fig. 9 displays the time dependence of the stationary nutations  $M_{Y_1}^S$  of the ketone signal before, during and after modulated photolysis ( $\nu_m = 0.96 \nu_1$ ). From this it is evident that enhanced absorption is present during the whole irradiation period.

A complete spectrum of di-tert-butyl ketone during photolysis taken by the method of stationary nutations is presented as part (b) of fig. 2. If com-



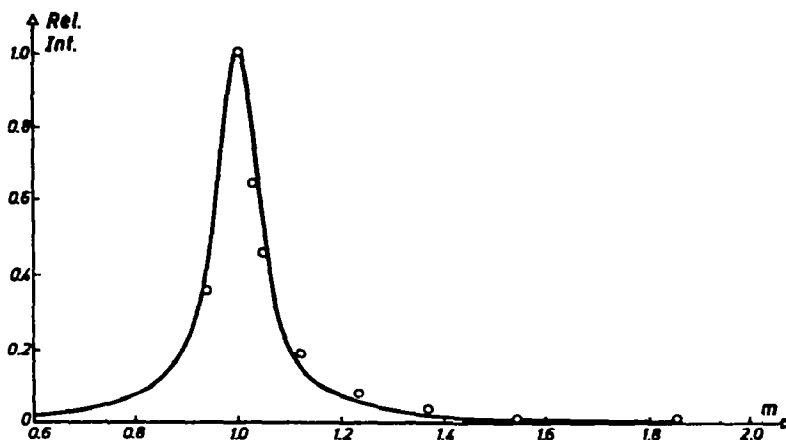


Fig. 6. Amplitude of the out-of-phase term  $M_{Y1}^S$  at resonance as a function of the modulation frequency  $\nu_m = m\nu_1$ . Data taken from fig. 4. Solid line calculated.

pared with the conventional spectrum of fig. 2a the individual lines appear slightly broader, but it is evident from the multiplets of isobutene 3 that the resolution is the same. There are several significant differences of the patterns of figs. 2a and 2b. In particular, the relative intensities of the polarizations of the groups are different. We believe that this is due to the different dependence of steady state and stationary nutation CIDNP-signals on the relaxation times. The amplitudes of the former are directly proportional to  $T_1$  if recorded under conditions of negligible saturation [see eq. (13)] so that in groups

with long  $T_1$  the effects will appear overemphasized whereas groups with small  $T_1$  show only minor polarization. On the other hand, the stationary nutation signals do not depend on  $T_1$  if  $T_1 \gg T_2$  [see eq. (16)]. We therefore conclude that the relative intensities of the single lines in fig. 2b represent a better picture of the formation rates of polarization than those of fig. 1a. Furthermore, the relative amplitudes of the isobutene 3  $\text{CH}_2$ -transitions at  $\delta = 4.47$  ppm have a different appearance for the two modes of detection. In fig. 2a five of the seven

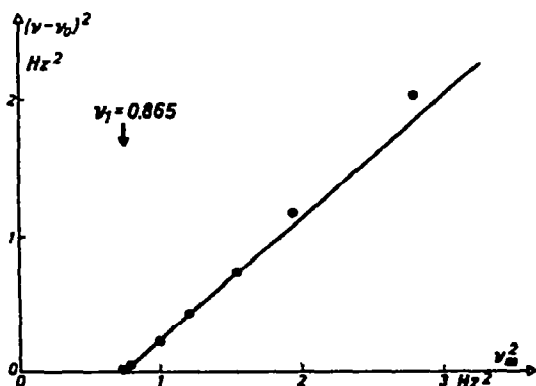


Fig. 7. Splitting of  $M_{Y1}^S$  for  $m > 1$  as function of the modulation frequency. Data taken from fig. 4. Solid line calculated.

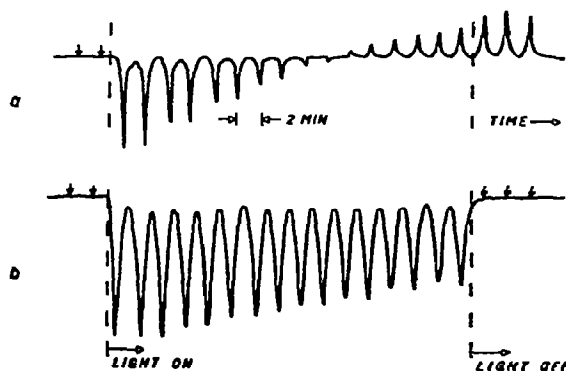


Fig. 8. NMR-signal of tert-butyl chloride versus time of photolysis: (a) continuous photolysis, (b) nutation signal  $M_{Y1}^S$  during modulated photolysis  $\nu_m = 0.92\nu_1$  (1 denotes resonance positions).

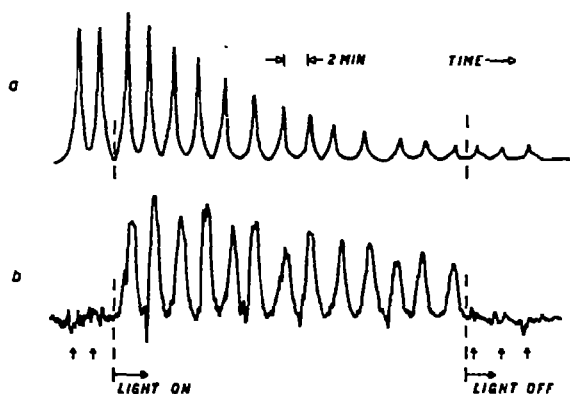


Fig. 9. NMR-signal of di-tert-butyl ketone versus time of photolysis: (a) continuous photolysis, (b) nutation signal  $MS_{y1}$  during modulated photolysis  $\nu_m = 0.92\nu_1$  (↑ denotes resonance positions).

lines show enhanced absorption whereas in fig. 2b enhanced absorption is evident for three and emission for two of the lines. Since the relative amplitudes of multiplets in steady state spectra may be influenced by inter- and intramolecular relaxation effects [28, 29] we again believe that the multiplet in fig. 2b represents the true CIDNP-pattern to a better extent.

## 5. Conclusions

We have shown that transient nutations of magnetization occur if a magnetization is generated with a constant rate at resonance. They are observed in photochemically induced dynamic nuclear polarization. If the reaction rate is modulated at or near the nutation frequency stationary nutations result which allow a phase sensitive detection. The effects are explained quantitatively by Bloch-type equations and can be used to discriminate polarized from unpolarized parts of CIDNP-spectra. The stationary nutations technique may have as a most important application the detection of weak polarization of reaction products of CIDNP-signals which are superposed on nonpolarized lines such as solvents or nonpolarized reagents. The results of this study also demonstrate that at least for single line spectra the nutation amplitudes are often unaffected by longitudinal relaxation and thus represent the polarization rates more

directly than steady state spectra. Very probably the relative amplitudes of CIDNP-multiplets are also less distorted by relaxation effects and we shall investigate this feature more fully in the future.

## Acknowledgement

We appreciate helpful discussions on the photo-CIDNP of di-tert-butyl ketone with Dr. B. Blank of this institute, and are grateful for support by the Jubiläumsspende für die Universität Zürich and the Swiss National Foundation for Scientific Research.

## References

- [1] B. Winkler-Lardelli, H.J. Rosenkranz, H.-J. Hansen, H. Schmid, B. Blank and H. Fischer, *Helv. Chim. Acta* 56 (1973) 2628.
- [2] W. Adam, J. Arce de Sanabria and H. Fischer, *J. Org. Chem.* 38 (1973) 2571.
- [3] W. Adam, H. Fischer, H.-J. Hansen, H. Heimgartner, H. Schmid and H.-R. Waespe, *Angew. Chem.* 85 (1973) 669.
- [4] H.C. Torrey, *Phys. Rev.* 76 (1949) 1059;
- [5] R.G. Brewer and R.L. Shoemaker, *Phys. Rev. Letters* 27 (1971) 631; 28 (1972) 1430.
- [6] G.B. Hocker and C.L. Tang, *Phys. Rev. Letters* 21 (1968) 591.
- [7] J.H.-S. Wang, J.M. Levy, S.G. Kukolich and J.I. Steinfeld, *Chem. Phys.* 1 (1973) 141.
- [8] A. Abragam, *Principles of magnetic resonance* (Clarendon, Oxford, 1961).
- [9] D. Ziessow and E. Lippert, *Ber. Bunsenges. Physik. Chem.* 74 (1970) 335.
- [10] J.S. Leigh Jr., *Rev. Sci. Instr.* 39 (1968) 1594.
- [11] J.A. Ferretti and R. Freeman, *J. Chem. Phys.* 44 (1966) 2054.
- [12] D. Ziessow, *J. Chem. Phys.* 55 (1971) 984.
- [13] N.C. Verma and R.W. Fessenden, *J. Chem. Phys.* 58 (1973) 2501.
- [14] P.W. Atkins, K.A. McLauchlan and P.W. Percival, *Mol. Phys.* 25 (1973) 281.
- [15] M. Tomkiewicz, A. Groen and M. Cocivera, *Chem. Phys. Letters* 10 (1971) 39.
- [16] M. Tomkiewicz, A. Groen and M. Cocivera, *J. Chem. Phys.* 56 (1972) 5850.
- [17] B. Blank, A. Henne and H. Fischer, *Helv. Chim. Acta*, in press.
- [18] F.J. Adrian, *J. Chem. Phys.* 54 (1971) 3912.
- [19] R. Kaptein, *J. Am. Chem. Soc.* 94 (1972) 6251.
- [20] G.T. Evans, P.D. Fleming and R.G. Lawler, *J. Chem. Phys.* 58 (1973) 2071.

- [21] G.L. Closs, *J. Am. Chem. Soc.* 92 (1970) 2186.
- [22] H. Fischer, *Topics Current Chem.* 24 (1971) 1.
- [23] M. Kasha, *J. Opt. Soc. Am.* 38 (1948) 929.
- [24] H. Paul and H. Fischer, *Helv. Chim. Acta* 56 (1973) 1575.
- [25] W.A. Anderson, in: *NMR and EPR spectroscopy* (Pergamon, Oxford, 1960).
- [26] R. Kaptein, *Chem. Commun.* (1971) 732.
- [27] J.A. den Hollander, R. Kaptein and P.A.T.M. Brand, *Chem. Phys. Letters* 10 (1971) 430.
- [28] K. Müller and G.L. Closs, *J. Am. Chem. Soc.* 94 (1972) 1002.
- [29] M. Lehnig and H. Fischer, *Z. Naturforsch.* 27a (1972) 1300.